

Available online at www.sciencedirect.com

SciVerse ScienceDirect

<http://www.elsevier.com/locate/biombioe>

Comparative techno-economic analysis of biohydrogen production via bio-oil gasification and bio-oil reforming

Yanan Zhang^a, Tristan R. Brown^b, Guiping Hu^c, Robert C. Brown^{a,b,*}

^a Department of Mechanical Engineering, Iowa State University, Bioeconomy Institute, 1140 E BRL Building, Ames, IA 50011, USA

^b Bioeconomy Institute, Iowa State University, Ames, IA 50011, USA

^c Industrial and Manufacturing Systems Engineering, Iowa State University, Ames, IA 50011, USA

ARTICLE INFO

Article history:

Received 13 September 2012

Received in revised form

10 January 2013

Accepted 13 January 2013

Available online 14 February 2013

Keywords:

Fast pyrolysis

Bio-oil

Reforming

Gasification

Biohydrogen

ABSTRACT

This paper evaluates the economic feasibility of biohydrogen production via two bio-oil processing pathways: bio-oil gasification and bio-oil reforming. Both pathways employ fast pyrolysis to produce bio-oil from biomass stock. The two pathways are modeled using Aspen Plus[®] for a 2000 t d^{−1} facility. Equipment sizing and cost calculations are based on Aspen Economic Evaluation[®] software. Biohydrogen production capacity at the facility is 147 t d^{−1} for the bio-oil gasification pathway and 160 t d^{−1} for the bio-oil reforming pathway. The biomass-to-fuel energy efficiencies are 47% and 84% for the bio-oil gasification and bio-oil reforming pathways, respectively. Total capital investment (TCI) is 435 million dollars for the bio-oil gasification pathway and is 333 million dollars for the bio-oil reforming pathway. Internal rates of return (IRR) are 8.4% and 18.6% for facilities employing the bio-oil gasification and bio-oil reforming pathways, respectively. Sensitivity analysis demonstrates that biohydrogen price, biohydrogen yield, fixed capital investment (FCI), bio-oil yield, and biomass cost have the greatest impacts on facility IRR. Monte-Carlo analysis shows that bio-oil reforming is more economically attractive than bio-oil gasification for biohydrogen production.

© 2013 Elsevier Ltd. All rights reserved.

1. Introduction

Growing concerns over greenhouse gas (GHG) emissions from the combustion of fossil fuels have prompted interest in the production of hydrogen from biorenewable sources (biohydrogen). Unlike conventional hydrogen, which is produced from fossil fuel feedstocks such as natural gas, biohydrogen is a “carbon-neutral” product in that GHGs emitted during its combustion are offset by those sequestered during the biomass feedstock growth cycle. Biohydrogen can replace fossil

fuel-based hydrogen in the refining, petrochemical, food, and electronics industries [1]. Currently hydrogen is an important input in the upgrading of heavy petroleum fractions to high-value products such as gasoline and diesel fuel. U.S. petroleum production is expected to steadily increase over the next two decades as unconventional petroleum sources such as oil shale and tar sands come online [2]. These unconventional sources are frequently heavier than conventional sources and require additional hydroprocessing prior to refining into gasoline and diesel fuel. When the necessary hydrogen is derived

* Corresponding author. Department of Mechanical Engineering, Iowa State University, Bioeconomy Institute, 1140 E BRL Building, Ames, IA 50011, USA. Tel.: +1 515 294 7934; fax: +1 515 294 3091.

E-mail address: rcbrown@iastate.edu (R.C. Brown).

0961-9534/\$ – see front matter © 2013 Elsevier Ltd. All rights reserved.

<http://dx.doi.org/10.1016/j.biombioe.2013.01.013>

from fossil fuel sources, the lifecycle GHG emissions for these products increase substantially relative to those for products from conventional petroleum. These lifecycle emissions can be alleviated in part through the use of biohydrogen during hydroprocessing, leading biohydrogen to play an important role in mitigating the GHG emissions associated with unconventional petroleum sources.

Gasification and pyrolysis of biomass feedstocks are promising pathways for the commercial-scale production of biohydrogen [3]. While the production of biohydrogen via direct gasification of biomass is technically feasible [4–9], the low bulk density of the biomass feedstock results in a high feedstock cost [10]. In addition, bio-oil is cleaner than the biomass feedstock because many of the minerals and metals found in the latter are concentrated in the product char, which is separated from the product biohydrogen [11]. For these reasons bio-oil produced via biomass fast pyrolysis is a promising feedstock for biohydrogen production.

Several previous studies have examined the production of biohydrogen via steam reforming of bio-oil [12–21]. A variety of catalysts have been investigated for their suitability in the steam reforming of bio-oil including Ni-supported alumina catalysts, noble metals, zeolites, and mixed metal catalysts such as Pt/ZrO₂. Bio-oil composition, pyrolysis reactor type, and biomass feedstock types are also considered to be key factors in biohydrogen production via steam reforming of bio-oil [22–25]. Experimental studies of biohydrogen production via bio-oil gasification include both catalytic and non-catalytic gasification in fluidized beds and pressurized entrained-flow gasification [10,11,26–30]. A number of techno-economic studies of bio-oil gasification to produce a variety of fuels and commodity chemicals have been reported [31–33].

Researchers have also estimated the cost of hydrogen production via steam reforming of bio-oil. Sarkar and Kumar [34] analyzed a 2000 t d⁻¹ fast pyrolysis and steam reforming facility for the production of biohydrogen from bio-oil derived from whole trees, forest residues, and straw at projected costs of 2.40 \$ kg⁻¹ (20 \$ GJ⁻¹ of H₂), 3.00 \$ kg⁻¹ (25 \$ GJ⁻¹ of H₂), and 4.55 \$ kg⁻¹ of H₂ (38 \$ GJ⁻¹ of H₂), respectively. Kinoshita and Turn [35] modeled a smaller bio-oil-to-biohydrogen system using CaO as a CO₂ sorbent. They found that the biohydrogen yield from the sorbent-aided system is comparable to that predicted for catalytic steam reforming of bio-oil without the use of sorbents, producing 0.07–0.08 kg H₂ per kg of bio-oil.

This study investigates the economic feasibility of two pathways for biohydrogen production from bio-oil produced via biomass fast pyrolysis. Both a bio-oil reforming process and a bio-oil gasification process are modeled with Aspen Plus

and the 20-year facility IRRs are calculated to quantify the economic feasibility of each pathway. Finally, the sensitivity of the facility IRRs to different parameters is reported along with the results of a Monte-Carlo uncertainty analysis.

2. Process design

This study simulates two pathways for biohydrogen production via bio-oil processing: bio-oil gasification and bio-oil reforming. Both pathways employ fast pyrolysis to produce bio-oil from a biomass feedstock. The gasification and fast pyrolysis models used in this study are based on models developed as part of a joint study by Iowa State University, the National Renewable Energy Laboratory, and ConocoPhillips that received extensive external review before publication as NREL design reports [36,37]. The bio-oil production process includes the areas of biomass preprocessing, fast pyrolysis, solids removal, bio-oil recovery, bio-oil storage, and combustion. The generalized process diagram for the two pathways is shown in Fig. 1.

In the biomass preprocessing area the biomass moisture content is reduced from 25% to 7% and ground to a particle size with a diameter of 3 mm. Preprocessing consists of biomass drying and size reduction. Steam rotary dryers are used to dry the biomass due to their wide application and long history in industries. Primary particle size reduction simulates grinding of biomass to particle size of about 10 mm. Secondary particle size reduction simulates a hammer mill producing particles averaging 3 mm. The energy requirement for size reduction is calculated from the correlations developed by Mani et al. [38]. Corn stover is selected as the biomass feedstock as investigated by the previous pyrolysis-based biofuels production techno-economic analysis (see Table 1) [39]. Corn stover pyrolysis analysis is modified from USDA experimental data [40] and Char composition analysis is from the sample based on Iowa State University laboratory results [39,41].

In the pyrolysis area the preprocessed biomass is converted to raw bio-oil via fast pyrolysis. A fluidized bed reactor is employed as the pyrolyzer operating at 500 °C and 1 atm. The RYield module in Aspen Plus is used to simulate the pyrolyzer in conjunction with data on bio-oil and non-condensable gases obtained from a previous pyrolysis-based biofuels production techno-economic analysis (see Table 2) [39]. In the combustion area the non-condensable gases (NCGs) and a fraction of the char produced during fast pyrolysis are combusted to supply process heat for the pyrolysis reactor. Then the combusted gases serve as a recycled

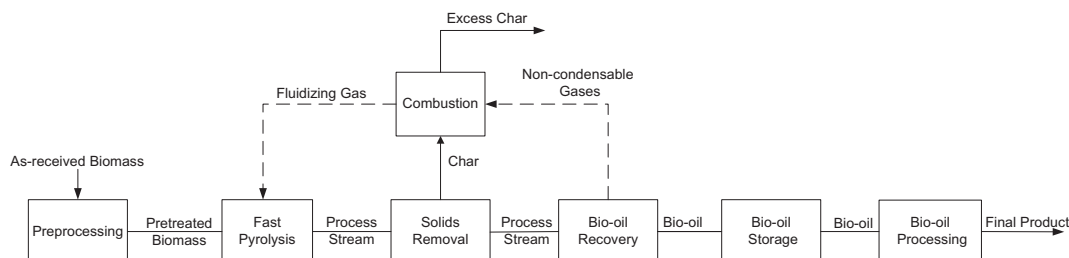


Fig. 1 – Generalized process flow diagram for the two pathways.

Table 1 – Ultimate and proximate analyses for corn stover feedstock and char (mass fraction) [39].

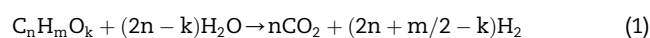
Ultimate analysis			Proximate analysis		
Element	Corn stover (dry basis)	Char (dry basis)	Element	Corn stover (wet basis)	Char (dry, ash-free)
Carbon	47.28	51.2	Moisture	25.0	0
Hydrogen	5.06	2.12	Fixed Content	17.7	51.21
Nitrogen	0.8	0.45	Volatile Matter	52.8	49.79
Chlorine	0	0.471	Ash	4.5	0
Sulfur	0.22	0.935			
Oxygen	40.63	11.5			
Ash	6	33.3			

fluidized agent carrying the heat for pyrolysis process. The raw bio-oil is purified by removing the entrained particles (ash and char) through the cyclones with efficiency of 90%, then condensed and stored in the bio-oil recovery and storage areas. In bio-oil recovery areas, the electrostatic precipitators (ESP) and condensers are used to collect the aerosols and condense the vapor compounds to liquid phase. This bio-oil production from biomass fast pyrolysis process design is similar to those used in previous studies [39,42,43].

In the first pathway, bio-oil and excess biochar is gasified with steam and oxygen (95% purity) in a slagging entrained flow gasifier operating at a temperature of 1200 °C and a pressure of 20 bar to produce syngas (see Fig. 2). The RGibbs model used to model the gasifier is based on minimizing the Gibbs free energy with phase splitting. The oxygen employed for bio-oil gasification is generated through an air separation unit (ASU). A slag separator is employed to separate the generated slag from the product syngas. The high temperature gases exiting the slag separator are cooled in a recovery steam cycle. After heat recovery, the gases are sent to a sour water gas shift (SWGS) reactor where CO and water are converted to hydrogen and CO₂ at 700 °C. After that, the gases go to a direct quench system where the char, dissolved ammonia and ammonium chloride are removed along with the contaminated water. The direct quench system reduces the gases to around 40 °C. After quenching, the gas stream is sent to a monoethanolamine-based acid gas removal system that removes a portion of the CO₂ and H₂S from the syngas [44]. Hydrogen sulfide, carbonyl sulfide and ammonia exiting

syngas cleanup area are $8.3 \times 10^{-7} \text{ mg m}^{-3}$, $3.1 \times 10^{-2} \text{ mg m}^{-3}$ and 0.12 mg m^{-3} , respectively. Carbon dioxide occupies 6% in the syngas. After cleaning, another water gas shift (WGS) reactor operating at 450 °C is employed to produce more hydrogen from the adjusted syngas. A pressure swing adsorption (PSA) system is employed to recover high purity hydrogen from the shifted syngas, which is modeled by Sep module. The recovered hydrogen is compressed and stored for further use. The low pressure PSA tail gas stream is separated into three streams. One stream is recycled to the WGS reactor to improve the conversion efficiency and one stream goes to the acid gas removal system as another recycle stream. The third stream serves as fuel gas for heat generation.

Nickel-based catalytic steam reforming of bio-oil is investigated in the second pathway (see Fig. 3). The collected bio-oil is first sent to a pre-reformer mixer with high temperature steam. The mass ratio of steam to liquid bio-oil is 1:1 (kg kg⁻¹). In the pre-reformer, water-gas-shift reaction and steam methane reforming reactions take place. Then the stream is sent to the reformer to produce hydrogen by catalytic steam reforming. The steam reforming reaction mechanism used in the reformer is based on Marquovich et al. [45]. The general reaction in the reformer is described as:



The specific reactions modeled in reformer are shown in Table 3. Thermodynamic equilibrium calculations indicate that the bio-oil compounds of acetic acid and ethylene glycol can be fully reformed even at low temperatures [46], which allows the reformer to be modeled with an REquil module with assumed operating temperature of 700 °C. All of these reactions are assumed to be simultaneous and reach equilibrium at the specified temperature. A heat exchanger is employed between the pre-reformer and the reformer for the purpose of heat recovery. After the reforming step, the product gases enter a quench vessel where they are cooled down. In the hydrogen recovery step a PSA is employed to separate the hydrogen from the exiting gases. The hydrogen separated via the PSA is then sent to a hydrogen storage area while the other gases are combusted to provide process heat.

Table 2 – Pyrolysis products distribution (mass fraction of corn stover feedstock) [39].

Bio-oil composition		Gases	
Water	10.8	Nitrogen	0
Acetic acid	5.93	Carbon dioxide	5.42
Propionic acid	7.31	Carbon monoxide	6.56
Methoxyphenol	0.61	Methane	0.035
Ethylphenol	3.80	Ethane	0.142
Formic acid	3.41	Hydrogen	0.588
Propyl-benzoate	16.36	Propene	0.152
Phenol	0.46	Ammonia	0.0121
Toluene	2.27	Total	12.91
Furfural	18.98		
Benzene	0.77	Solids	
Total	70.7	Char/Ash	16.39

3. Economic analysis

Aspen Economic Evaluation[®] software and literature data are employed to estimate modeled equipment costs for the bio-oil

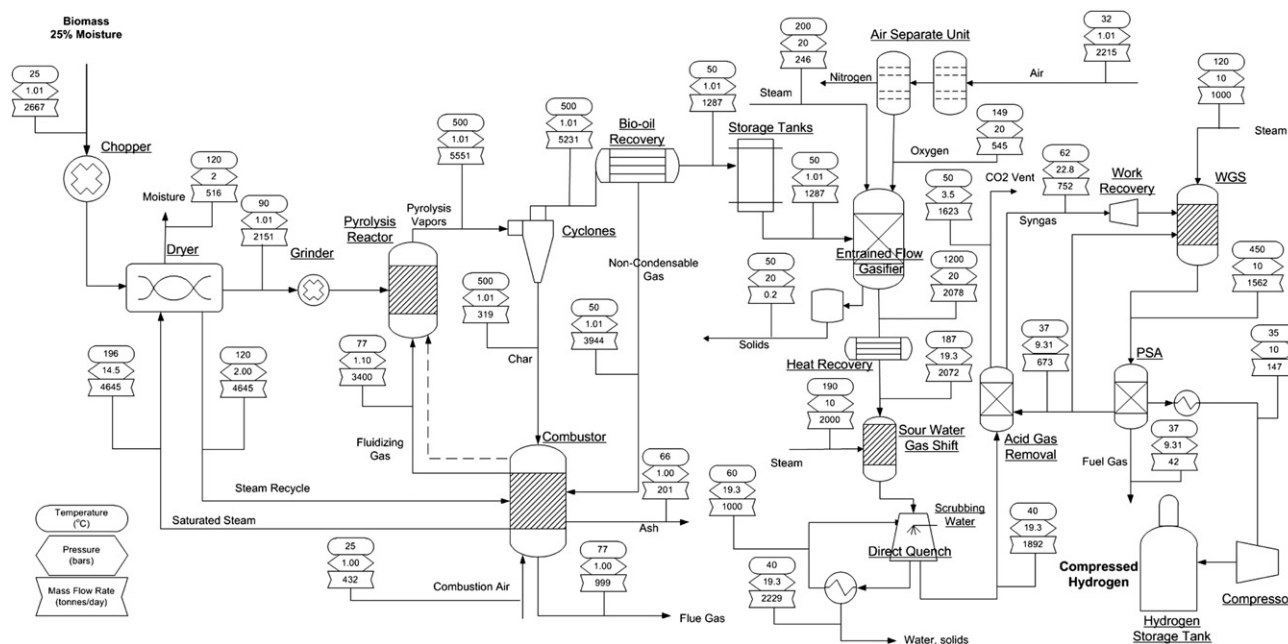


Fig. 2 – Overall process flow diagram for the bio-oil gasification pathway.

gasification and bio-oil reforming pathways. For equipment cost estimation of the pyrolysis reactor, it is assumed that four 500 t d^{-1} fluidized bed reactors are employed. Equipment cost analysis for the pyrolysis reactor and steam reformer is made with Aspen Economic Analyzer [36]. Unit costs for several unique units, such as the entrained flow gasifier, are calculated from base equipment costs by employing equipment scaling exponents and cost year index factors. Equation (2) is employed to calculate the scaled equipment cost, where C_{new}

is the scaled new equipment cost, C_0 is the base equipment cost, S_{new} is the new equipment size, S_0 is the base equipment size, n is the scaling exponent for a particular type of equipment, I_0 is the base year index and I is the calculated year index.

$$C_{\text{new}} = (I/I_0) * C_0 * (S_{\text{new}}/S_0)^n \quad (2)$$

The scaling factor typically ranges from 0.6 to 0.8. For entrained flow gasifiers, n is assumed to be 0.7 and the base

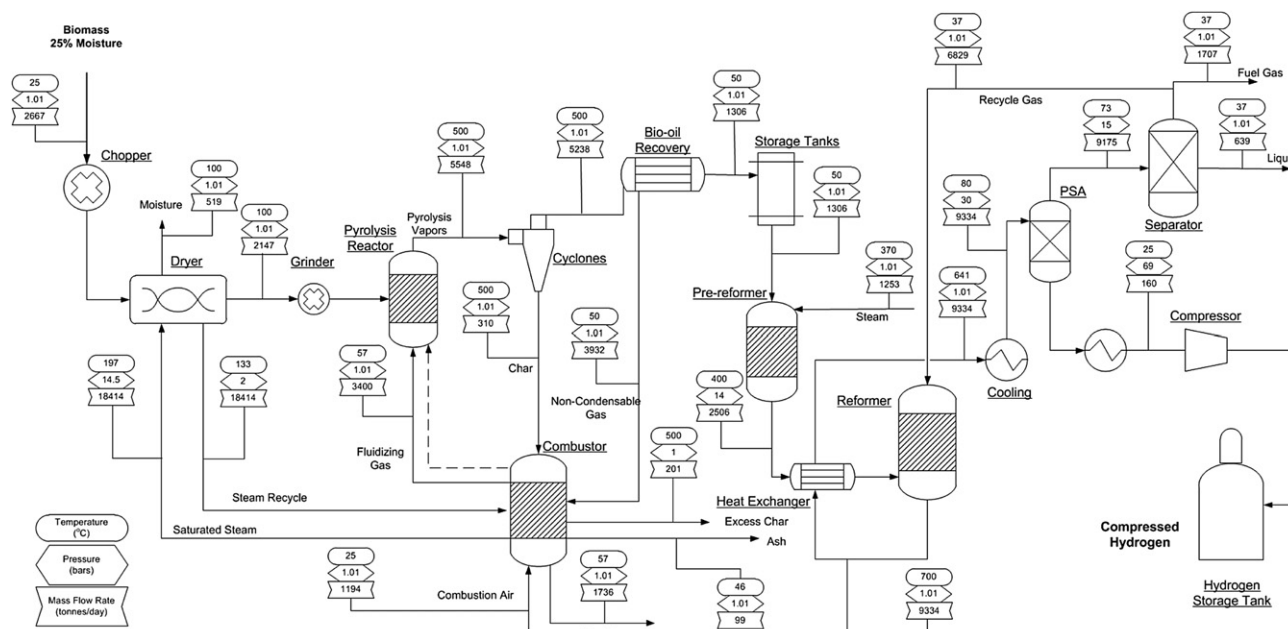


Fig. 3 – Overall process flow diagram for the bio-oil reforming pathway.

Table 3 – Simulated steam reforming reactions in the reformer.

Number	Reaction
1	$C_2H_4O_2 \rightarrow 2H_2 + 2CO$
2	$C_3H_6O_2 + 4H_2O \rightarrow 7H_2 + 3CO_2$
3	$C_7H_8O_2 + 12H_2O \rightarrow 16H_2 + 7CO_2$
4	$C_5H_4O_2 + 8H_2O \rightarrow 10H_2 + 5CO_2$
5	$C_6H_8O_2 + 10H_2O \rightarrow 14H_2 + 6CO_2$
6	$C_6H_6O + 11H_2O \rightarrow 14H_2 + 6CO_2$
7	$CH_2O_2 \rightarrow H_2 + CO_2$
8	$CH_4O + H_2O \rightarrow 3H_2 + CO_2$
9	$CO + H_2O \rightarrow CO_2 + H_2$
10	$CO + 3H_2 \rightarrow CH_4 + H_2O$
11	$CH_4 + H_2O \rightarrow CO + 3H_2$
12	$CH_2O_2 \rightarrow H_2O + CO$

year is 2006. For the high pressure ammine system, n is assumed to be 0.75 and the base year is 2005. For sour water gas shifter reactor, n is assumed to be 0.71 and the base year is 2007. The scaling factor and base equipment cost come from a previous analysis [37,47]. All cost estimations are based on 2010 dollars for economic calculation.

A capital cost estimation methodology developed by Peters et al. [48] for calculating installation costs is employed (see Table 4). A total installation factor of 3.02 is used to estimate the installed equipment costs for solid–liquid chemical facilities [48]. A Lang Factor of 5.46, which has been employed in previous analyses of pyrolysis-based biofuels production [39], is employed to estimate total capital investment (TCI). This analysis assumes an n th plant operating for 20 years based on the current state of technology.

Table 5 details the variable operating cost assumptions used in this analysis. The parameters for electricity, hydrogen, and char are based on the average EIA 20-year price forecasts for each [2]. In the case of char, this value is calculated by treating it as a low-value coal substitute (as low as one-half that of coal) in power facilities for electricity generation

Table 4 – Methodology for capital cost estimation for n^{th} facility.

Parameter	Assumption
Total Purchased Equipment Cost (TPEC)	100%
Purchased Equipment Installation	39%
Instrumentation and Controls	26%
Piping	10%
Electrical Systems	31%
Buildings (including services)	29%
Yard Improvements	12%
Service Facilities	55%
Total Installed Cost (TIC)	$3.02 \times \text{TPEC}$
Indirect Cost (IC)	$0.89 \times \text{TPEC}$
Engineering	32%
Construction	34%
Legal and Contractors Fees	23%
Total Direct and Indirect Costs (TDIC)	$\text{TIC} + \text{IC}$
Contingency	20% of TDIC
Fixed Capital Investment (FCI)	$\text{TDIC} + \text{Contingency}$
Working capital (WC)	15% of FCI
Land Use	6% of TPEC
Total Capital Investment (with land)	$\text{FCI} + \text{WC} + \text{Land}$

Table 5 – Material and operating parameters employed in the evaluation.

Material	Price
Feedstock	$83 \$ t^{-1}$
Electricity	$0.061 \$ kWh^{-1}$ [2]
Process Water	$0.032 \$ t^{-1}$
Steam	$9.05 \$ t^{-1}$
Catalyst	11.77 million $\$ yr^{-1}$ [52]
Solids Disposal Cost	$19.84 \$ t^{-1}$
Waste Water Disposal Cost	$1.16 \$ t^{-1}$
Fuel Gas	$1.06 \$ GJ^{-1}$
Hydrogen	$3.33 \$ kg^{-1}$ [2]
Char	$18.21 \$ t^{-1}$ [2]

based on the 20-year price forecast for coal [2,49]. The corn stover feedstock is assumed to be purchased for $83 \$ t^{-1}$, which is in line with existing facility-gate cost estimates for forest thinnings and logging residues [50,51]. The solids disposal cost and waste water disposal cost are based on the NREL gasification design report [37]. In addition to the above variable operating costs, fixed operating costs including labor salaries, overhead, maintenance, insurances and taxes are estimated. Maintenance and insurance costs are assumed to be 1.5% and 2% of total fixed capital investment. Labor salaries are adapted from the NREL report [36] and overhead is assumed to be 60% of labor costs.

A discounted cash flow rate of return (DCFRROR) spreadsheet is employed to determine the facility internal rate of return (IRR). Table 6 details the major assumptions employed in DCFRROR analysis.

4. Results

4.1. Process modeling

For both pathways, the biomass feedstock has 25% moisture content, which is reduced to 7% after drying. Pyrolysis yields

Table 6 – Assumptions for DCFRROR analysis.

Parameter	Assumption
Working Capital (% of FCI)	15%
Salvage Value	0
Type of Depreciation	DDB
General Plant	200
Steam Plant	150
Depreciation Period (Years)	
General Plant	7
Steam/Electricity System	20
Construction Period (Years)	2.5
% Spent in Year –3	8%
% Spent in Year –2	60%
% Spent in Year –1	32%
Start-up Time (Years)	0.5
Revenues (% of Normal)	50%
Variable Costs (% of Normal)	75%
Fixed Cost (% of Normal)	100%
Income Tax Rate	39%
Facility Type	n^{th} facility

wet bio-oil with moisture content of 20%. Assuming the yield of wet bio-oil from dry biomass is 63%, then a fast pyrolysis plant processing 2000 t d⁻¹ dry corn stover will yield 1260 t d⁻¹ of bio-oil (wet basis). Biohydrogen yield for the bio-oil gasification and bio-oil reforming pathways are 147 t d⁻¹ and 160 t d⁻¹, representing 11.7% and 12.7% of wet bio-oil, respectively.

The input–output mass and energy balances based on low heating value (LHV) for the two pathways are shown in Table 7. Biohydrogen is the main energy output as measured by net energy output of 735 GJ h⁻¹ and 800 GJ h⁻¹ for bio-oil gasification pathway and bio-oil reforming pathway. For bio-oil gasification pathway, 70% of the char is combusted to heat the pyrolysis reactor and the rest of the char is sent to the entrained flow gasifier. For bio-oil reforming pathway, fuel gas is the second largest net energy output at 270 GJ h⁻¹. Of the char product, 33% is combusted for process heat and the rest of the char contributes 18% of the total net energy output for this pathway. The overall biomass to fuels energy efficiency for bio-oil gasification and bio-oil reforming pathway facility on LHV basis is approximate 47% and 84%, respectively.

4.2. Economics results

Estimated installed equipment costs for a 2000 t d⁻¹ facility are 241 million dollars for the gasification pathway and 184 million dollars for the reforming pathway. Total capital investment (TCI) is the sum of total installed equipment cost, working capital cost, total indirect cost, land use and project contingency (see Table 4). The installed equipment cost for the bio-oil gasification facility is greater than that of bio-oil reforming facility, which contributes to the 102 million dollars difference in TCI for the two facilities. Detailed capital costs for the two pathways are shown in Table 8.

Fig. 4 details the breakdown of the installed equipment costs according to model area. The installed equipment costs for the preprocessing, combustion, pyrolysis and oil recovery, storage, and utilities areas are identical for the gasification and reforming pathways. However, the bio-oil gasification process requires greater capital investment in the bio-oil processing area for three reasons. First, the entrained flow gasifiers employed for bio-oil gasification are much more expensive than the reformers employed for bio-oil reforming. Second, the gasification pathway requires a syngas cleanup stage that incurs additional capital costs. Third, bio-oil gasification employs oxygen as the gasification agent, requiring

Table 8 – Capital costs for bio-oil gasification and bio-oil reforming pathways (million dollars).

Costs	Bio-oil gasification	Bio-oil reforming
Total Installed Equipment Cost	241	184
Working Capital	56	43
Total Indirect Cost	71	54
Project Contingency	62	48
Land Use	5	4
Total Capital Investment	435	333

installation of an ASU. Because of these differences, the total installed cost for the bio-oil gasification pathway is 31% higher than for the bio-oil reforming pathway.

Total annual operating costs (see Fig. 5) are calculated on the basis of stream mass flows in the Aspen Plus model and the current market prices of the products for the two pathways (see Table 3). In both pathways the feedstock cost is the largest contributor to operating costs, at 54 million dollars annually. However, capital depreciation and income tax are quite different for the two pathways. Capital depreciation is 19 million dollars and 14 million dollars respectively for the bio-oil gasification and bio-oil reforming pathways. Capital depreciation is directly related to capital investment. The annual income tax burden is 12 million dollars for the gasification pathway and 25 million dollars for the reforming pathway. In this case greater net revenue results in a larger income tax burden.

Based on the calculated capital costs, operating costs, and output values, a facility IRR of 8.4% and 18.6% is calculated for the bio-oil gasification and bio-oil reforming pathways, respectively. This result shows that bio-oil reforming process has better economic feasibility than the bio-oil gasification process for production of biohydrogen.

5. Discussion

Fig. 6 summarizes the variation in facility IRRs at different capacities for bio-oil gasification and bio-oil reforming facilities. The bio-oil reforming pathway has much higher facility IRRs for biohydrogen production than gasification at any output; however, the overall trend in facility IRRs in relation to facility capacity is similar for both pathways. Facility IRR increases rapidly when facility size increases from 500 to

Table 7 – Mass and energy balance for biohydrogen production via two pathways.

Pathway	Bio-oil gasification			Bio-oil reforming		
	Mass (t d ⁻¹)	LHV (MJ kg ⁻¹)	Energy (GJ h ⁻¹)	Mass (t d ⁻¹)	LHV (MJ kg ⁻¹)	Energy (GJ h ⁻¹)
In						
Biomass	2000	18	1500	2000	18	1500
Electricity	n/a	n/a	82.4	n/a	n/a	48.7
Out						
Hydrogen	147	120	735	160	120	800
Char	0	27.5	0	205.6	27.5	236
Fuel gas	42	1.5	2.6	1707	3.8	270

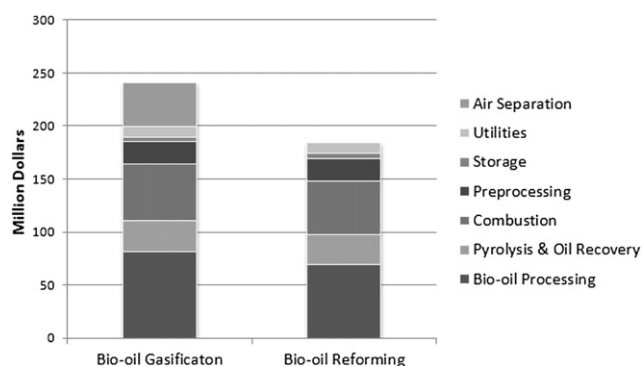


Fig. 4 – Installed equipment costs for two biohydrogen production pathways.

2000 t d⁻¹ but at a slower rate beyond 2000 t d⁻¹. Facility IRR for the bio-oil gasification pathway increases rapidly from -8.2% to 8.6% as facility size increases from 500 to 2000 t d⁻¹. A minimum facility size is therefore necessary to generate a positive IRR for the bio-oil gasification pathway. IRR for a facility employing the bio-oil reforming pathway follows a similar trend but has a higher starting point, with IRR increasing from 10.3% to 18.6% when facility capacity increases from 500 to 2000 t d⁻¹. This shows that the bio-oil reforming pathway is still economically feasible even at much smaller scale. The difference in IRRs between a 500 t d⁻¹ facility and a 10000 t d⁻¹ facility is 17.6% and 29.7% for bio-oil reforming and bio-oil gasification, respectively.

The results of a sensitivity analysis for both the gasification and reforming pathways are presented to demonstrate the sensitivity of facility IRR to parameter values. The parameters investigated are biohydrogen price, biohydrogen yield, biomass cost, FCI, bio-oil yield, facility maintenance cost, income tax rate, and working capital cost for both pathways. The analysis finds that facility IRR for both pathways is most sensitive to biohydrogen price, biohydrogen yield, FCI, bio-oil yield, and biomass cost (see Fig. 7 and Fig. 8).

Biohydrogen is the main product for both pathways so its yield and market price have a significant impact on facility IRR. For the gasification pathway, a negative facility IRR occurs if the biohydrogen price reaches its lower bound of 2.33 \$ kg⁻¹

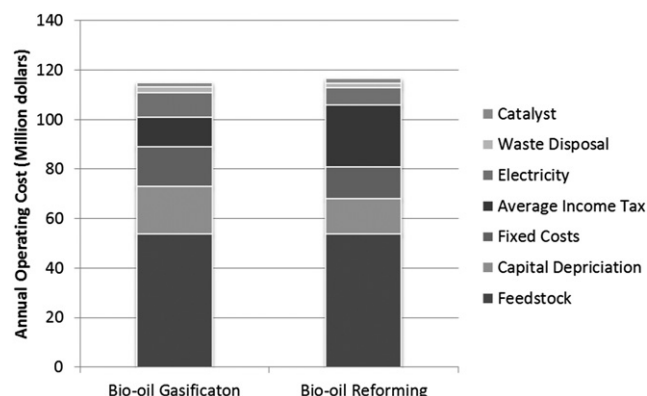


Fig. 5 – Annual operating costs for gasification and reforming pathways.

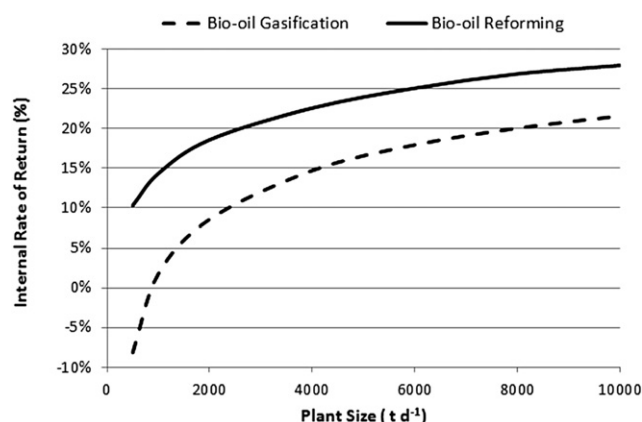


Fig. 6 – Variation of facility IRR with facility size for bio-oil gasification and bio-oil reforming pathways.

whereas an IRR of 15.6% is obtained with an upper bound hydrogen price of 4.33 \$ kg⁻¹. Increasing the biohydrogen yield from 9.4% to 14% (mass fraction of wet bio-oil) could increase facility IRR from 2.3% to 13.4%. A $\pm 30\%$ range in FCI and biomass cost results in a facility IRR range of 5.9–12.4% and 5.0–11.4%, respectively.

The bio-oil reforming pathway has a higher biohydrogen yield (12.7% vs. 11.7% mass fraction of wet bio-oil) and lower FCI (286 million dollars vs. 374 million dollars), so the facility IRR range under the reforming pathway is much larger (8.9%–26.2%) than that of the bio-oil gasification pathway (-2.6%–15.7%). These results show that biohydrogen production via bio-oil reforming is much more economically feasible than biohydrogen production via bio-oil gasification, with a comparatively low investment risk.

A Monte-Carlo simulation for facility IRR distribution is conducted using Crystal Ball[®] software to quantify the uncertainty of the bio-oil reforming pathway's result. Biohydrogen price, biohydrogen yield, FCI, and biomass cost are treated as changing variables in a Monte-Carlo simulation since these parameters have the greatest impact on facility IRR. All of these variables are assumed to follow triangular distributions with the same variation ranges used in the sensitivity analysis (see Figs. 7 and 8). Two thousand random facility IRRs are generated during the Monte-Carlo simulation and JMP[®] software is employed to analyze the resulting data.

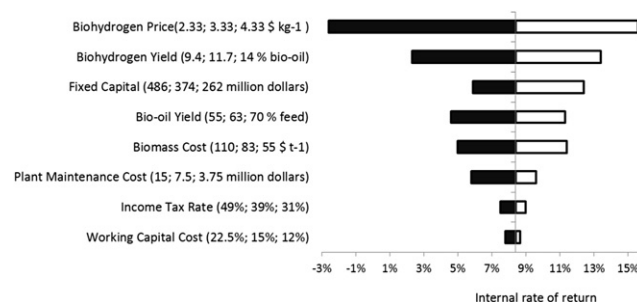


Fig. 7 – Sensitivity analysis for the bio-oil gasification pathway.

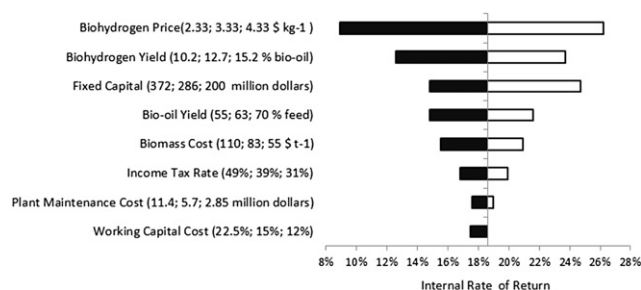


Fig. 8 – Sensitivity analysis for the bio-oil reforming pathway.

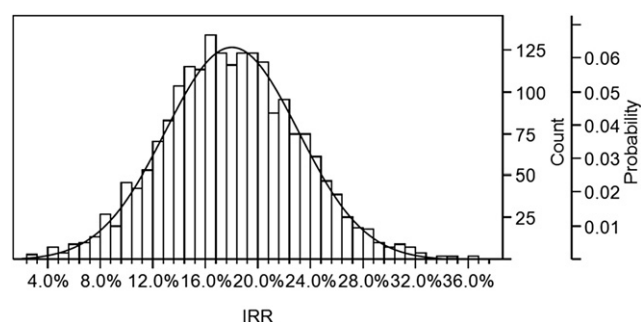


Fig. 9 – Facility IRR distribution from Monte-Carlo simulation.

Fig. 9 details the facility IRR distribution from the Monte-Carlo simulation. The expected value of the mean facility IRR is 17.9% and the standard deviation is 5.0%. The minimum IRR is 2.9% and the maximum IRR is 36.5%. The median, 25% quartile, and 75% quartile facility IRRs are 14.5%, 17.9% and 21.4%, respectively. For the cumulative probability distribution of the facility IRR, more than 94% of facilities in the analysis have IRRs exceeding 10% and 34% of facilities will have IRRs exceeding 20% (see Fig. 10). This result shows that

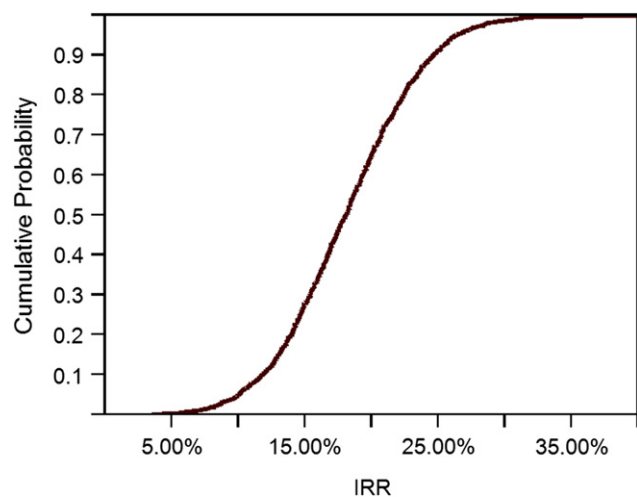


Fig. 10 – Cumulative probability distribution of facility IRR from Monte-Carlo simulation.

biohydrogen via bio-oil reforming is likely to be economically feasible even considering a wide range of possible cost and performance parameters.

6. Conclusions

This techno-economic analysis (TEA) compares the economic feasibility of biohydrogen production via bio-oil gasification and bio-oil reforming. Facility internal rate of return (IRR) is calculated as a function of annual revenues, fixed capital investment (FCI), and annual operating costs. In this study the technology is assumed to be mature enough from the perspectives of reliability and performance to ensure that the facility operates as an nth rather than pioneer plant.

Based on a 2000 t d⁻¹ facility, annual biohydrogen production capacity is calculated to be 147 t d⁻¹ for the bio-oil gasification pathway and 160 t d⁻¹ for the bio-oil reforming pathway. Bio-oil reforming pathway has higher hydrogen yield because all the bio-oil compounds can be catalytic reformed to hydrocarbons. In addition, hydrogen yield could be increased by water gas shift reaction. The estimated total fixed capital investment (FCI) for a facility employing the bio-oil gasification pathway is 374 million dollars with total capital investment (TCI) of 435 million dollars. Total FCI for a facility employing the bio-oil reforming pathway is 286 million dollars and TCI is 333 million dollars. The capital cost investment for bio-oil gasification is greater than for bio-oil reforming pathway. This is mainly because entrained flow gasifiers are much more expensive than reformers. In addition, bio-oil gasification requires air separation equipment and more complicated syngas cleanup system. The 20-year IRR is calculated to be 8.4% for a facility employing the bio-oil gasification pathway and 18.6% for a facility employing the bio-oil reforming pathway.

A sensitivity analysis is performed to determine the sensitivity of the facility's economic feasibility to model parameters. Sensitivity analysis shows that hydrogen price, hydrogen yield, FCI, feedstock cost, and bio-oil yield are key factors in the economic feasibility of biohydrogen production via both the bio-oil gasification and bio-oil reforming pathways. The lower facility IRR for the bio-oil gasification pathway relative to the bio-oil reforming pathway is primarily due to the former's lower yield of biohydrogen and higher TCI. Facility IRR ranges from -2.6% to 15.6% for the bio-oil gasification pathway and 8.9%–26.2% for the bio-oil reforming pathway. A Monte-Carlo simulation of biohydrogen production via bio-oil reforming shows that more than 94% of facilities will have IRRs exceeding 10% and 34% of facilities will have IRRs exceeding 20% based on 2000 random runs of the simulation. This indicates that the risk for investing in biohydrogen production via the bio-oil reforming pathway is relatively low. Compared to biohydrogen production via the bio-oil gasification pathway, the bio-oil reforming pathway has advantages including lower TCI and higher biohydrogen yields. However, fouling from coke formation is a potential problem for the reforming pathway, requiring additional research to overcome this problem. The gasification pathway has higher capital costs and lower energy efficiency than the reforming pathway.

Acknowledgments

We appreciate the support of the U.S. Department of Agriculture in performing this analysis under Grant No. 68-3A75-5-233.

REFERENCES

- [1] Milne TA, Elam CC, Evans RJ. Hydrogen from biomass: state of the Art and research Challenges. A report for the International energy Agency Agreement on the production and Utilization of hydrogen: Task 16, hydrogen from carbon-Containing Materials (IEA/H2/TR-02/001). Golden, CO: National Renewable Energy Laboratory; 2002. Report No.: TP-510–36262.
- [2] U.S. Energy Information Administration. Annual energy outlook 2011. Washington, DC; 2011. Report No: DOE/EIA-0383(2011).
- [3] Anghel M, Niculescu V, Stefanescu I, Tamaian R. Green technologies for sustainable hydrogen production. An impact study. In: Chemical, Biological and Environmental Engineering (ICBEE), 2010 2nd International Conference; 2010 Nov 2–4. p. 19–22.
- [4] Chang ACC, Chang H-F, Lin F-J, Lin K-H, Chen C-H. Biomass gasification for hydrogen production. *Int J Hydrogen Energy* 2011;36(21):14252–60.
- [5] Shen L, Gao Y, Xiao J. Simulation of hydrogen production from biomass gasification in interconnected fluidized beds. *Biomass and Bioenergy* 2008;32(2):120–7.
- [6] Kriengsak SN, Buczynski R, Gmurczyk J, Gupta AK. Hydrogen production by high-temperature steam gasification of biomass and coal. *Environ Eng Sci* 2009;26:739–44.
- [7] Song T, Wu J, Shen L, Xiao J. Experimental investigation on hydrogen production from biomass gasification in interconnected fluidized beds. *Biomass Bioenergy* 2012;36: 258–67.
- [8] Wei L, Xu S, Liu J, Liu C, Liu S. Hydrogen production in steam gasification of biomass with CaO as a CO₂ absorbent. *Energy Fuels* 2008;22:1997–2004.
- [9] Cohce MK, Rosen MA, Dincer I. Efficiency evaluation of a biomass gasification-based hydrogen production. *Int J Hydrogen Energy* 2011;36:11388–98.
- [10] Sakaguchi M, Watkinson AP, Ellis N. Steam gasification of bio-oil and bio-Oil/Char Slurry in a fluidized bed reactor. *Energy Fuels* 2010;24(9):5181–9.
- [11] van Rossum G, Kersten SRA, van Swaaij WPM. Catalytic and noncatalytic gasification of pyrolysis oil. *Ind Eng Chem Res* 2007;46:3959–67.
- [12] Basagiannis AC, Verykios XE. Steam reforming of the aqueous fraction of bio-oil over structured Ru/MgO/Al₂O₃ catalysts. *Catal Today* 2007;127:256–64.
- [13] Yan C-F, Cheng F-F, Hu R-R. Hydrogen production from catalytic steam reforming of bio-oil aqueous fraction over Ni/CeO₂-ZrO₂ catalysts. *Int J Hydrogen Energy* 2010;35:11693–9.
- [14] Vagia EC, Lemonidou AA. Thermodynamic analysis of hydrogen production via autothermal steam reforming of selected components of aqueous bio-oil fraction. *Int J Hydrogen Energy* 2008;33:2489–500.
- [15] Hou T, Yuan L, Ye T, Gong L, Tu J, Yamamoto M, et al. Hydrogen production by low-temperature reforming of organic compounds in bio-oil over a CNT-promoting Ni catalyst. *Int J Hydrogen Energy* 2009;34:9095–107.
- [16] Garcia L, French R, Czernik S, Chornet E. Catalytic steam reforming of bio-oils for the production of hydrogen: effects of catalyst composition. *Appl Catal A: Gen* 2000;201:225–39.
- [17] Domine ME, Iojoiu EE, Davidian T, Guilhaume N, Mirodatos C. Hydrogen production from biomass-derived oil over monolithic Pt- and Rh-based catalysts using steam reforming and sequential cracking processes. *Catal Today* 2008;133–135:565–73.
- [18] Czernik S, Evans R, French R. Hydrogen from biomass-production by steam reforming of biomass pyrolysis oil. *Catal Today* 2007;129(3–4):265–8.
- [19] Seyedein-Azad F, Salehi E, Abedi J, Harding T. Biomass to hydrogen via catalytic steam reforming of bio-oil over Ni-supported alumina catalysts. *Fuel Process Technol* 2011; 92(3):563–9.
- [20] Thaicharoensutcharittham S, Meeyoo V, Kitiyanan B, Rangsunvigit P, Rirksomboon T. Hydrogen production by steam reforming of acetic acid over Ni-based catalysts. *Catal Today* 2011;164(1):257–61.
- [21] Zhang S-p, Li X-j, Li Q-y, Xu Q-l, Yan Y-j. Hydrogen production from the aqueous phase derived from fast pyrolysis of biomass. *J Anal Appl Pyrolysis* 2011;92(1):158–63.
- [22] Chen T, Wu C, Liu R. Steam reforming of bio-oil from rice husks fast pyrolysis for hydrogen production. *Bioresour Technol* 2011;102(19):9236–40.
- [23] Ortiz-Toral PJ, Satrio J, Brown RC, Shanks BH. Steam reforming of bio-oil fractions: Effect of composition and Stability. *Energy Fuels* 2011;25:3289.
- [24] Mueller-Langer F, Tzimas E, Kaltschmitt M, Peteves S. Techno-economic assessment of hydrogen production processes for the hydrogen economy for the short and medium term. *Int J Hydrogen Energy* 2007;32(16):3797–810.
- [25] Liu S-m, Chen M-q, Wang J, Min F-f, Chen M-g. . Hydrogen production by steam reforming for glycerol as a model oxygenate from bio-oil. In: Materials for Renewable Energy & Environment (ICMREE), 2011 International Conference; 2011 May 20–22. p. 303–7.
- [26] Liu S-m, Chen M-q, Wang J, Chen M-g. . Gasification of acetic acid as a model oxygenate from bio-oil by Microwave heating. In: E-Product E-Service and E-Entertainment (ICEEE), 2010 International Conference; 2010 Nov 7–9. p. 1–4.
- [27] Marda JR, DiBenedetto J, McKibben S, Evans RJ, Czernik S, French RJ, et al. Non-catalytic partial oxidation of bio-oil to synthesis gas for distributed hydrogen production. *Int J Hydrogen Energy* 2009;34(20):8519–34.
- [28] Rennard D, French R, Czernik S, Josephson T, Schmidt L. Production of synthesis gas by partial oxidation and steam reforming of biomass pyrolysis oils. *Int J Hydrogen Energy* 2010;35(9):4048–59.
- [29] Demirbas MF. Hydrogen from Various biomass Species via pyrolysis and steam gasification processes. *Energy Sources, Part A: Recovery, Utilization, Environ Effects* 2006;28(3):245–52.
- [30] Chhiti Y, Salvador S, Commandré J-m, Broust Fo, Couhert C. Wood bio-oil Noncatalytic Gasification: Influence of temperature, Dilution by an Alcohol and ash content. *Energy Fuels* 2010;25(1):345–51.
- [31] Ng KS, Sadhukhan J. Techno-economic performance analysis of bio-oil based Fischer-Tropsch and CHP synthesis platform. *Biomass Bioenergy* 2011;35(7):3218–34.
- [32] Ng KS, Sadhukhan J. Process integration and economic analysis of bio-oil platform for the production of methanol and combined heat and power. *Biomass and Bioenergy* 2011; 35(3):1153–69.
- [33] Villanueva Perales AL, Reyes Valle C, Ollero P, Gómez-Barea A. Technoeconomic assessment of ethanol production via thermochemical conversion of biomass by entrained flow gasification. *Energy* 2011;36(7):4097–108.
- [34] Sarkar S, Kumar A. Large-scale biohydrogen production from bio-oil. *Bioresour Technol* 2010;101(19):7350–61.
- [35] Kinoshita CM, Turn SQ. Production of hydrogen from bio-oil using CaO as a CO₂ sorbent. *Int J Hydrogen Energy* 2003; 28(10):1065–71.

- [36] Wright MM, Satrio JA, Brown RC, Daugaard DE, Hsu DD. Techno-economic analysis of biomass fast pyrolysis to Transportation fuels. Golden, CO: National Renewable Energy Laboratory; 2010. Report No.: NREL/TP-6A20-46586.
- [37] Swanson RM, Satrio JA, Brown RC, Platon A, Hsu DD. Techno-economic analysis of biofuels production based on gasification. Golden, CO: National Renewable Energy Laboratory; 2010. Report No.: NREL/TP-6A20-46587.
- [38] Mani S, Tabil LG, Sokhansanj S. Grinding performance and physical properties of wheat and barley straws, corn stover and switchgrass. *Biomass and Bioenergy* 2004;27(4):339–52.
- [39] Wright MM, Daugaard DE, Satrio JA, Brown RC. Techno-economic analysis of biomass fast pyrolysis to transportation fuels. *Fuel* 2010;89(Supplement 1):S2.
- [40] Mullen CA, Boateng AA, Goldberg NM, Lima IM, Laird DA, Hicks KB. Bio-oil and bio-char production from corn cobs and stover by fast pyrolysis. *Biomass and Bioenergy* 2010;34(1): 67–74.
- [41] Rover M. In: Wright M, editor. Pyrolysis bio-oil and char analysis sample #2006-27; 2008.
- [42] Brown TR, Zhang Y, Hu G, Brown RC. Techno-economic analysis of biobased chemicals production via integrated catalytic processing. *Biofuels, Bioproducts and Biorefining* 2012;6(1):73–87.
- [43] Brown TR, Wright MM, Brown RC. Estimating profitability of two biochar production scenarios: slow pyrolysis vs fast pyrolysis. *Biofuels, Bioproducts and Biorefining* 2011;5(1):54–68.
- [44] Nexant Inc. Equipment design and cost estimation for small modular biomass systems, synthesis gas cleanup, and oxygen separation equipment. Golden, CO: National Renewable Energy Laboratory; 2006. Report No.: NREL/SR-510-39945.
- [45] Markevich M, Czernik S, Chornet E, Montané D. Hydrogen from biomass: steam reforming of model compounds of fast-pyrolysis oil. *Energy Fuels* 1999;13(6):1160–6.
- [46] Ortiz-Toral PJ. Steam reforming of bio-oil: Effect of bio-oil composition and stability. United States–Iowa: Iowa State University; 2008.
- [47] Swanson RM. Techno-economic analysis of biomass-to-liquids production based on gasification. United States – Iowa: Iowa State University; 2009.
- [48] Peters MS, Timmerhaus KD, West RE. Plant design and economics for chemical engineers. New York: McGraw-Hill; 2003.
- [49] McCarl BA, Peacocke C, Chrisman R, Kung C-C, Sands RD. Economics of biochar production, utilization and greenhouse gas offsets. In: Lehmann J, Joseph S, editors. *Biochar for Environmental Management*. London: Earthscan; 2009. p. 341.
- [50] Committee on Economic and Environmental Impacts of Increasing Biofuels Production and National Research Council. Renewable fuel standard: potential economic and Environmental Effects of U.S. Biofuel Policy. Washington, D.C: The National Academies Press; 2011.
- [51] Department of Energy. U.S. Billion-Ton Update: biomass supply for a Bioenergy and Bioproducts Industry. Oak Ridge, TN: Oak Ridge National Laboratory; 2011. Report No.: ORNL/TM-2011/224.
- [52] Meyers R. Handbook of petroleum refining processes. New York: McGraw-Hill; 1997.